RevMexAA (Serie de Conferencias), **9**, 210–212 (2000)

MHD MODELS FOR PNE

G. García-Segura,[1] J. Franco,[1] J. A. López,[1] N. Langer,[2] and M. Różyczka[3]

RESUMEN

Se presenta un escenario auto consistente para explicar la morfología de las nebulosas planetarias. El escenario es consistente con la distribución Galáctica de los diferentes tipos morfológicos. Este trabajo resuelve, por medio de efectos MHD, algunas de las características controversiales que aparecen en las nebulosas planetarias. Estas características incluyen la presencia de flujos axisimétricos y colimados, con una cinemática que aumenta linealmente con la distancia y la existencia de morfologías asimétricas tales como las de las nebulosas con simetría de punto.

ABSTRACT

A self-consistent scenario to explain the morphology of planetary nebulae is presented. This scenario is consistent with the Galactic distribution of different nebular types. This work addresses several controversial features that appear in planetary nebulae, which are easily solved by the inclusion of MHD effects. These features include the presence of axisymmetric and collimated outflows with linearly increasing kinematics, and the existence of asymmetrical morphologies such as point-symmetric nebulae.

Key Words: **ISM: JETS AND OUTFLOWS — MHD — PLANETARY NEBULAE: GENERAL**

1. INTRODUCTION

Planetary nebulae (PNe) display a rich variety of shapes, and have been cataloged in a series of morphological classes: bipolar, elliptical, point-symmetric, irregular, spherical and quadrupolar (Chu, Jacoby, & Arendt 1987; Schwarz, Corradi, & Melnick 1992; Stanghellini, Corradi, & Schwarz 1993; Manchado et al. 1996a, 1996b). In contrast, except for a few cases, dust shells around AGB stars do not show signs of asphericity (Bujarrabal & Alcolea 1991; Kahane & Jura 1994). Thus, during the transition from the AGB to the post-AGB phase, one or more physical processes responsible for the shape of these objects must be initiated. The origin of aspherical nebulae still remains as one of the fundamental problems of PNe formation and evolution (see reviews by Pottasch 1984; Iben 1993). Numerical simulations that reproduce PNe shapes have helped to gain insight into the basic physics acting in the formation of the different morphologies that are commonly observed in PNe. The two-wind model proposed by Kwok, Purton, & Fitzgerald (1978) has been applied and refined in a number of numerical simulations based on hydrodynamic models (e.g., Kahn & West 1985; Mellema, Eulderink, & Icke 1991; Frank & Mellema 1994; Dwarkadas, Chevalier, & Blondin 1996).

The main nebular morphologies are usually well reproduced in the hydrodynamic models; however, the production of jets and ansae have met with certain difficulties. In particular, fast winds do not tend to converge into stable structures to form them (e.g., Dwarkadas & Balick 1997). On a somewhat different approach, Chevalier & Luo (1994) have explored the effects of a rotating star with a magnetized wind on the formation of aspherical bubbles. Following this scheme, Różyczka & Franco (1996) and García-Segura et al. (1997; 1999), have performed 2D MHD simulations of this magnetized wind in cylindrical and spherical calculations, respectively, showing that magnetic tension can indeed be responsible for the generation of jets

[1]Instituto de Astronomía, Universidad Nacional Autónoma de México.
[2]Institut für Physik, Universität Potsdam, Germany.
[3]N. Copernicus Astronomical Center and Interdisciplinary Center for Mathematical and Computational Modeling, Poland.

in PNe. Recently, García-Segura (1997) presented full 3D MHD models of PNs where jets and ansae are convincingly reproduced as the result of magnetic collimation of the post-AGB wind.

A particularly intriguing case in PN morphologies are those that display point-symmetric structures. These have been recognized in a wide variety of PNe (Manchado et al. 1996a; Guerrero, Vázquez, & López 1999). In some particular instances, where reliable kinematical information is available, the presence of bipolar, rotating, episodic jets or BRETS have been inferred to explain similar structures (cf. López 1997).

In this paper, we discuss some features that are easily solved by MHD effects. In § 2 we describe the production of axisymmetric flows and the production of jets and ansae, with linearly increasing kinematics in the collimated outflows. In § 3 we discuss solutions for the special case of point-symmetric nebulae.

2. AXISYMMETRIC FLOWS

Axisymmetric flows can be produced by a magnetized wind with or without the existence of an equatorial density enhacement (EDE; see García-Segura et al. 1999 for examples). The magnetic field at the surface of a post-AGB star can be transported out by its wind, like in the solar wind case. Because of stellar rotation, the magnetic field in the wind is dominated by a toroidal component. The resulting toroidal field has a magnetic tension associated with it (Chevalier & Luo 1994; Contopoulos 1995). Thus, the general effect of the magnetic tension is the elongation of the nebula in the polar direction (Różyczka & Franco 1996).

2.1. *Confinement of Flows: Jets and Ansae*

Although the hoop stress is always present in this type of flows, the conditions to form observable jets are not always met. The result of varying the mass loss rate of the fast wind from large values to lower values is quite important for jet formation/detection.

Figure 1 (see Plate 1) shows the appreciable difference between three models E1, E2, and E3. The polar, piled-up gas in model E1 (higher value of $\dot{M}$) is able to cool down efficiently in a dynamical time scale comparable to the computed time. This feature results in "easily" detectable jets. In model E2 (moderate $\dot{M}$) the cooling is less efficient but still present, giving rise to the formation of ansae. Model E3 does not show any apparent signs of piled-up gas. Since these models have energy conserving dynamics (as imposed by the magnetic pressure) rather than momentum conserving, these estimations for the mass loss rates are quite independent of the terminal wind velocities. Note that, in the absence of magnetic fields, winds of the order of 100 km s^{-1} have strongly radiative terminal or reverse shocks (see, for example, Frank, Balick, & Livio 1996), and the radiative conditions are strongly dependent on the wind velocity and not only on the mass loss rate.

2.2. *Linearly Increasing Kinematics of the Collimated Outflows*

In order to verify if the MHD models can reproduce the range of observed velocities we compare them with observations. Figure 6 in García-Segura et al. (1999) shows the expansion velocity of the jet that appears in their model U, as it would be observed with a synthetic slit covering only the jet positions (1–2 on the figure). The model has been tilted 45° for a qualitative comparison with MyCn 18. The left panel of their Figure 6 agrees quite well with Figure 3*a* in Bryce et al. (1997), although the model was not specifically intended to reproduce this nebula. The most remarkable feature is the approximately linear increase of the expansion velocity along the jet, which matches the actual echelle observations. This acceleration is produced by the relaxation of the magnetic pressure in the shocked region. For completeness, the middle and right panels in Figure 6 of García-Segura et al. (1999) display two synthetic images of the emission measure of the gas, which can also be compared with Figure 1 in Bryce et al. (1997). The qualitative agreement is striking.

3. SOLUTIONS FOR POINT-SYMMETRY: BINARY SYSTEMS

Since the toroidal magnetic field carried out by the wind is always perpendicular to the rotation axis of the central star, it is now tempting to include precession (scenario I) or a steady tilt (scenario II) in the rotational axis of the primary star in a binary system. In both cases, it is easy to imagine the topology of the magnetic field lines in such scenarios, i.e., multiple magnetic rings centered along the spin axis of the primary star.

Astrophysical Plasmas: Codes, Models, and Observations (Mexico City, 25-29 October 1999)
Editors: Jane Arthur, Nancy Brickhouse, & José Franco

In order to illustrate how the precession (scenario I) can produce interesting effects, we have computed a model (see Plate 1, Fig. 2, left) with a precession period of 1300 yr and a precession angle of 10°. In order to have a general picture of the effect caused by the tilt (scenario II), we have computed several models in which the tilt angle varies from low values, 5°, through middle values, 15°, to large values, 45° (Fig. 2, middle and right).

GGS is grateful to A. Manchado and M. Peimbert for useful discussions, and JF thanks Tom Hartquist for long discussions, at several bars in Leeds, about MHD effects. All the computations were performed with ZEUS-3D at the SGI Origin 2000 of the Instituto de Astronomía-UNAM. We thank Michael L. Norman and the Laboratory for Computational Astrophysics for the use of ZEUS-3D. JF ackowledges partial support by DGAPA-UNAM grant IN130698 and a R&D CRAY Research grant.

Astrophysical Plasmas: Codes, Models, and Observations (Mexico City, 25-29 October 1999)
Editors: Jane Arthur, Nancy Brickhouse, & José Franco

REFERENCES

Bryce, M., López, J. A., Holloway, A. J., & Meaburn, J. 1997, ApJ, 487, L161
Bujarrabal, V., & Alcolea J. 1991, A&A, 251, 536
Chevalier, R. A., & Luo, D. 1994, ApJ, 421, 225
Chu, Y.-H., Jacoby, G. H., & Arendt, R. 1987, ApJS, 64, 529
Contopoulos, J. 1995, ApJ, 450, 616
Dwarkadas, V. V., & Balick, B. 1997, BAAS, 191, 15.05
Dwarkadas, V. V., Chevalier, R. A., & Blondin, J. M. 1996, ApJ, 457, 773
Frank, A., & Mellema, G. 1994, A&A, 289, 937
Frank, A., Balick, B., & Livio, M. 1996, ApJ, 471, L53
García-Segura, G. 1997, ApJ, 489, L189
García-Segura, G., Langer, N., Różyczka, M., & Franco, J. 1999, ApJ, 517, 767
García-Segura, G., Langer, N., Różyczka, M., Mac Low, M.-M., & Franco, J. 1997, in IAU Symp. 180, Planetary Nebulae, ed. H. J. Habing & H. J. G. L. M. Lamers (Dordrecht: Kluwer), 226
Guerrero, M. A., Vázquez, R., & López, J. A. 1999, ApJ, 117, 967
Iben, I. Jr. 1993, in IAU Symp. 155, Planetary Nebulae, ed. R. Weinberger & A. Acker (Dordrecht: Kluwer), 587
Kahane, C., & Jura M. 1994, A&A, 290, 183
Kahn, F. D., & West, K. 1985, MNRAS, 212, 837
Kwok, S., Purton, C. R., & Fitzgerald, P. M. 1978, ApJ, 219, L125
López, J. A. 1997, in IAU Symp. 180, Planetary Nebulae, ed. H. J. Habing & H. J. G. L. M. Lamers (Dordrecht: Kluwer), 226
Manchado, A., Guerrero, M., Stanghellini, L., & Serra-Ricart, M. 1996a, The IAC Morphological Catalog of Northern Galactic Planetary Nebulae (Tenerife: Instituto de Astrofísica de Canarias)
Manchado, A., Stanghellini, L., & Guerrero, M. 1996b, ApJ, 466, L95
Mellema, G., Eulderink, F., & Icke, V. 1991, A&A, 252, 718
Pottasch, S. R. 1984, Planetary Nebulae: A Study of Late Stages of Stellar Evolution (Dordrecht: Reidel)
Różyczka, M., & Franco, J. 1996, ApJ, 469, L127
Schwarz, H. E., Corradi, R. L. M., & Melnick, J. 1992, A&AS, 96, 23
Stanghellini, L., Corradi, R. L. M., & Schwarz, H. E. 1993, A&A, 276, 463

G. García-Segura and J. A. López: Instituto de Astronomía-UNAM, Apartado Postal 877, 22800 Ensenada, B. C., México (ggs, jal@astrosen.unam.mx).
J. Franco: Instituto de Astronomía, UNAM, Apartado Postal 70-264, 04510 México, D. F., México (pepe@astroscu.unam.mx).
N. Langer: Institut für Physik, Universität Potsdam, D-14415 Potsdam, Germany (ntl@astro.physik.uni-potsdam.de).
M. Różyczka: N. Copernicus Astronomical Center, Bartycka 18, 00-716 Warszawa, Poland (mnr@camk.edu.pl).

Astrophysical Plasmas: Codes, Models, and Observations (Mexico City, 25-29 October 1999)
Editors: Jane Arthur, Nancy Brickhouse, & José Franco

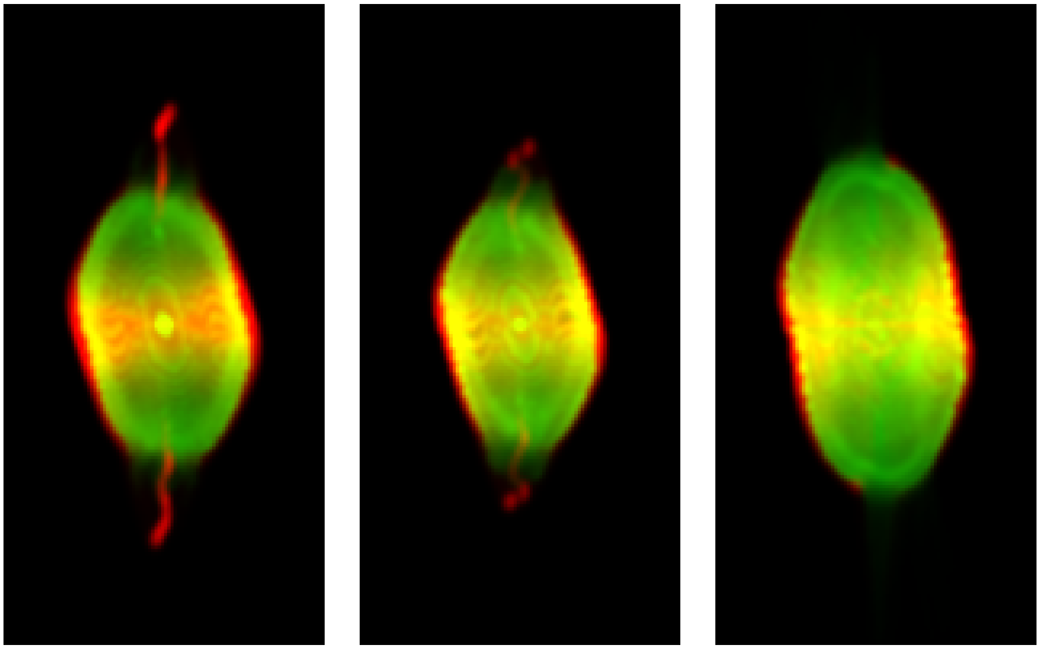

Fig. 1. Two-color, composite, synthetic images of the models. *Left*: E1 (1600 yr; $\dot{M} = 10^{-7}\ M_\odot$), *Middle*: E2 (1550 yr; $\dot{M} = 10^{-8}\ M_\odot$) and *Right*: E3 (2000 yr; $\dot{M} = 10^{-9}\ M_\odot$). Note the jet and the ansae in red (non-photoionized, shocked gas) as compared to the photoionized gas in green.

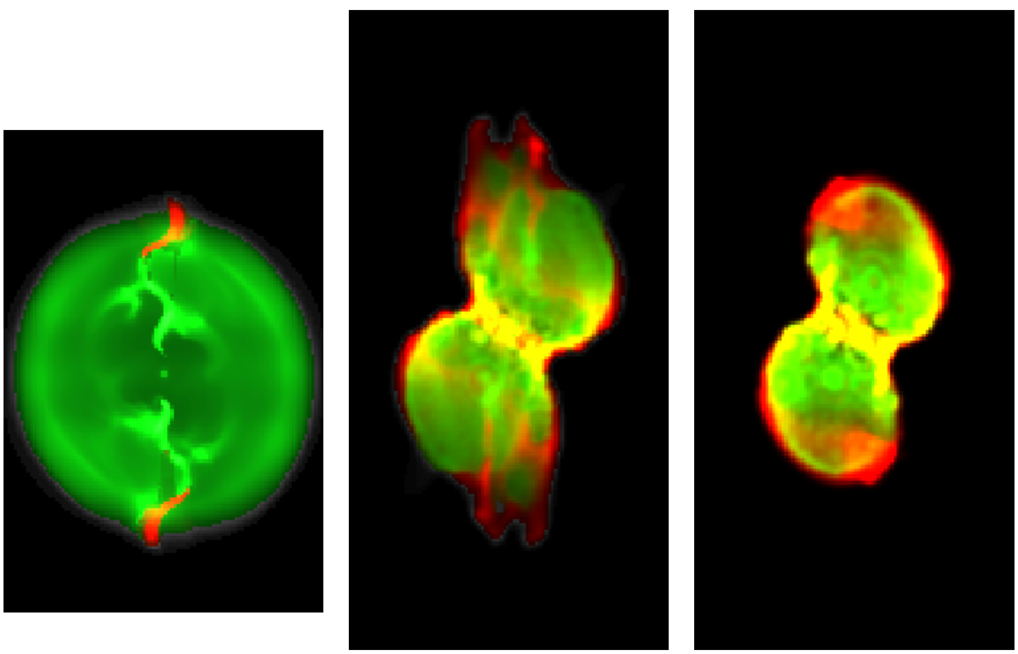

Fig. 2. *Left*: Scenario I. An example of a calculation which includes stellar precession ($P = 1300$ yr). *Middle and Right*: Scenario II. Examples of two calculations which include a steady tilt of 45°. Note again the jet and the ansae in red (non-photoionized, shocked gas) as compared to the photoionized gas in green.

GARCÍA-SEGURA ET AL. (see page 211)